H- Injection Simulations for a Multi-MW Upgrade

M. Hoppesch, J. Eldred, and D. Neuffer

August 12, 2021

Abstract

Fermilab intends to increase their beam power to 2.4 MW in an effort to advance the flagship long-baseline neutrino program. In [6] and [7] two scenarios are proposed for this "PIP-III" upgrade, a 2-8 GeV RCS or an 8 GeV Linac. A Python tracking simulation was developed to model foil injection for these cases. First, the simulation was matched to the well established PIP-II case. From the matched simulation, investigations established that an on-momentum longitudinal injection increases foil transverses in PIP-II. Then the simulation was changed to model the RCS and Linac PIP-III scenarios, for both correlated and anti-correlated beam painting. The results of the PIP-III studies indicate that correlated painting is preferable for both the Linac and RCS scenarios. This research creates a baseline of foil injection performance for PIP-III.

1 Introduction

1.1 Motivation

The Fermilab Long-Baseline Neutrino Detectors will benefit from production of a higher power proton beam. [2] The upcoming Proton Improvement Plan, known as PIP-II will implement a new 800 MeV Linac capable of delivering 1.2 MW of power. [1] To further increase beam power the Booster Ring, built in 1971, must be replaced. Two proposals are being considered for PIP-III, a 2 GeV Rapid Cycling Synchrotron (RCS) and an 8 GeV SRF Main Injector Linac (MI-Linac). [6] Designed to achieve a power of 2.4 MW, both proposals are demanding of H^- injection. The goal of this research was to simulate and optimize injection for these designs. Typically, injection is optimized when the stripping foil has minimal interactions with the already circulating beam. Too many foil interactions will eventually lead to mechanical failure as well as scattering losses.

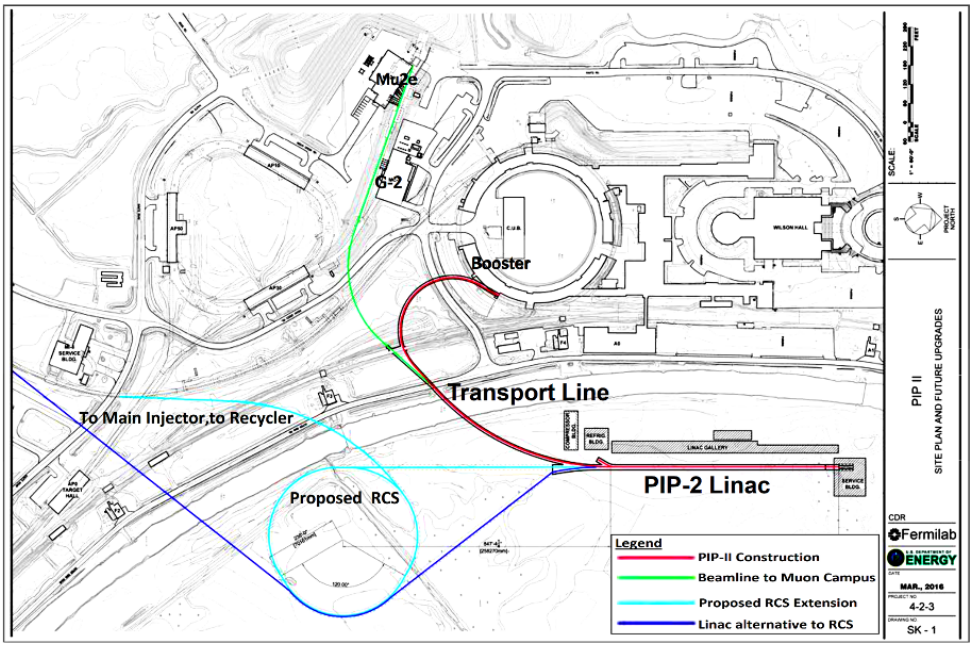

Figure 1: Schematic shows top view of Fermilab complex with PIP-II and both potential PIP-III sites

1.2 Background

Foil Stripping The accelerated protons begin their journey as H^- ions in the Linac. When they reach the end of the Linac, they are injected through a carbon foil into a ring. At this moment the H^- and proton encounter the foil, which strips the H^- electrons, resulting in only protons coming out the other side. Injection is performed in this manner to inject over multiple revolutions. If protons were injected, Liouville's Theorem would forbid injection of two protons into the same phase space. However, because an H^- and a proton have opposite charge, a magnetic gradient can be designed to bend the particles toward each other.

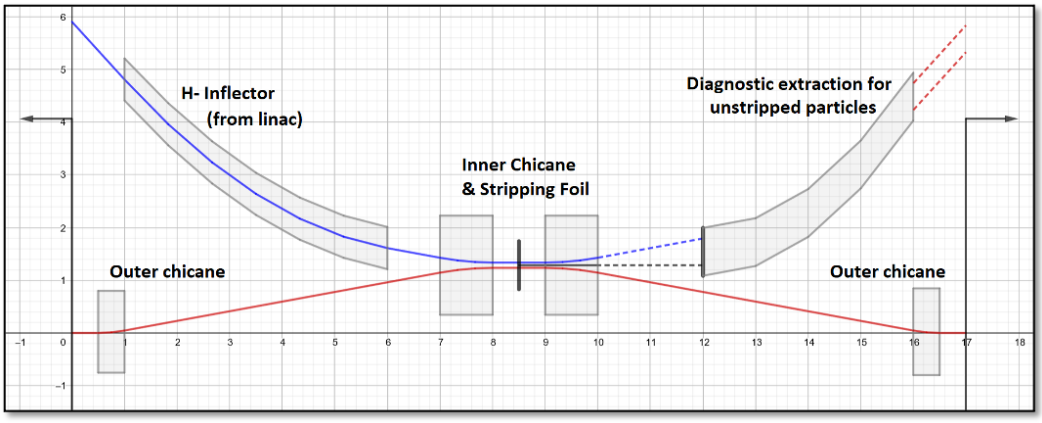

Figure 2: Basic Sketch of Foil Stripping Injection with (blue) H^- path, (red) p^+ beam path

For PIP-II the stripping foil thickness is 600 $\mu g/cm^2$. This is adequate to fully strip ($H^- \rightarrow p^+$) greater than 99.9 % of particles. [1] (This simulation is not concerned with the behavior of unstripped H^- ions.)

Beam Dynamics Transverse motion is determined by the Courant-Snyder parameters and the phase advance of the ring. [9] Since the point of interest is only the injection point, the Courant-Snyder parameters will be the same for the starting and ending points of the transformation that maps one whole turn. The phase advance for a whole ring is called the tune. For this simulation, the tune values of $Q_x = 0.425$ and $Q_y = 0.415$ were chosen to avoid resonance problems. Fig. 3 shows a final distribution using these tunes, which is well spread across phase space. With this framework, the phase space mapping of a particle can be determined by a transfer matrix, Eq. 1.

$$\begin{bmatrix} x_{n+1} \\ x'_{n+1} \end{bmatrix} = \begin{bmatrix} \cos 2\pi Q_x + \alpha_x \sin 2\pi Q_x & \beta_x \sin 2\pi Q_x \\ \frac{1+\alpha_x^2}{\beta_x} \sin 2\pi Q_x & \cos 2\pi Q_x - \alpha_x \sin 2\pi Q_x \end{bmatrix} \begin{bmatrix} x_n \\ x'_n \end{bmatrix} \tag{1}$$

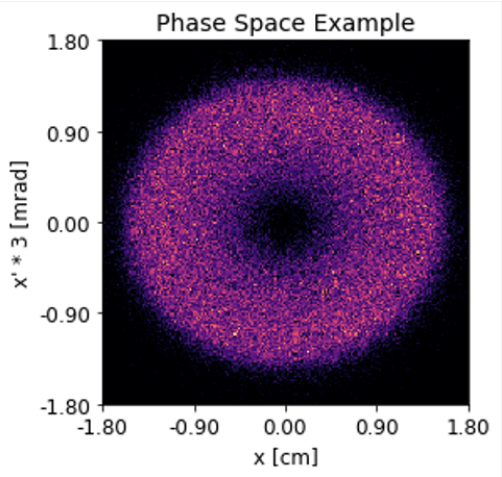

Figure 3: Phase Space Distribution Example

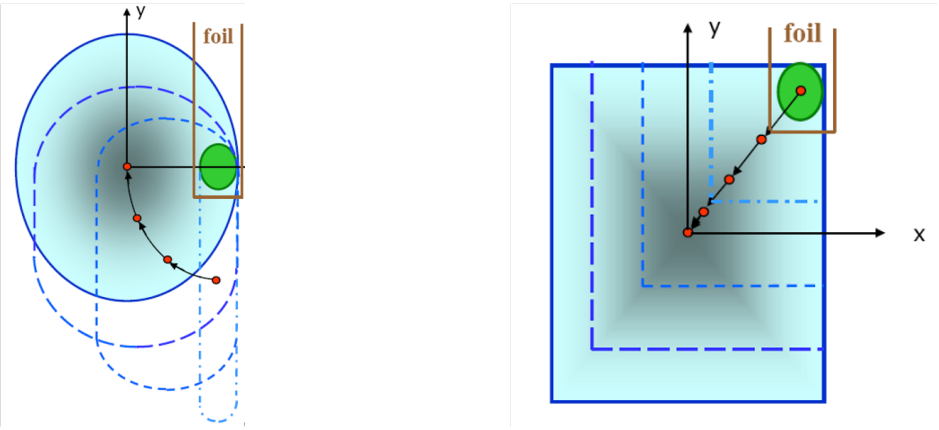

(a) Anti-correlated (b) Correlated

Figure 4: Different Possible Painting Schemes for PIP-III

Beam Painting The chicane magnets inside the injection region, Fig. 2, are responsible for moving the circulating beam relative to the foil. The advantage of this "painting" is that particles are not all injected into the same transverse space. Different kinds of painting schemes have different benefits and drawbacks. The two schemes investigated for PIP-III are a correlated and an anti-correlated painting, as shown in Fig. 4. One key difference in these two schemes is how the action of the particles changes throughout painting. The functional form for each painting is given by Eq. 2, from [10], for correlated painting and Eq. 3, from [1], for anti-correlated painting.

$$x(t) = x_{offset}\left[\sqrt{\left(\frac{t}{t_{inj}}\right)(1-\delta)+\delta}\right] \qquad y(t) = y_{offset}\left[\sqrt{\left(\frac{t}{t_{inj}}\right)(1-\delta)+\delta}\right] \tag{2}$$

$$x(t) = x_{offset}\cos\left[\left(\frac{\pi}{2}-\phi\right)\left(\frac{t}{t_{inj}}\right)+\phi\right]] \qquad y(t) = y_{offset}\sin\left[\left(\frac{\pi}{2}-\phi\right)\left(\frac{t}{t_{inj}}\right)+\phi\right]] \tag{3}$$

The distance that the Linac paints over is referred to as the painting offset. The correlated painting implements a square root function to achieve more uniform painting, as well as reduced foil hits. δ adjusts the starting point of the correlated painting, creating a slight hole in the middle of the final distribution. This avoids particles bunched in the center of the beam, where space charge could potentially create problems. This is important because correlated-painted beams will not maintain their form under transverse coupling. ϕ is a phase adjustment that ensures a more uniform anti-correlated painting. In said painting, particles are injected along the outside of an ellipse so most particles will have a similar action. Conversely, the correlated painting injects particles with small to large actions. [3] The Linac beam can paint over an area that will fill the geometric emittance, Eq. 4, of the ring.

$$\epsilon_{x,g,rms} = \frac{\epsilon_{x,n,rms}}{\beta_0\gamma_0} \tag{4}$$

Even though the Linac beams at 2 GeV and 8 GeV have the same normalized emittance, the 8 GeV beam will be injected into a smaller transverse space due to its smaller geometric emittance. Therefore, the 8 GeV foil will be subject to a higher density of primary hits.

Injection Mismatch In the absence of dedicated collimation, the Linac beam is normally distributed, and the number of primary particles that miss the foil will be dependent on foil size. In the PIP-II CDR the size is such that 99 % of particles hit the foil. [1] The spread of the beam is determined by the Courant-Snyder β parameter and the geometric emittance.

$$\sigma_x = \sqrt{\beta_s \epsilon_{x,g,rms}} \tag{5}$$

The number of secondary foil interactions is proportional to the size of the foil. In order to decrease the physical size of the foil, β_{Linac} must decrease. Injection mismatch is the ratio $\xi = \beta_{Linac}/\beta_{Ring}$. In SNS [4] and the PIP-II CDR [1] this parameter is considered optimal when Eq. 6 is met.

$$\xi = \frac{\beta_{Linac}}{\beta_{Ring}} = \left(\frac{\epsilon_{Linac}}{\epsilon_{Ring}}\right)^{1/3} \tag{6}$$

When the mismatch is less than this the concern is that the ring emittance will be determined more by the injection mismatch than the painting offset. [4]. For the PIP-III scenarios, this mismatch was studied by simulating injection at varying ξ, Fig. 5. The results of this parameter scan were fairly consistent over different painting schemes and injection energies.

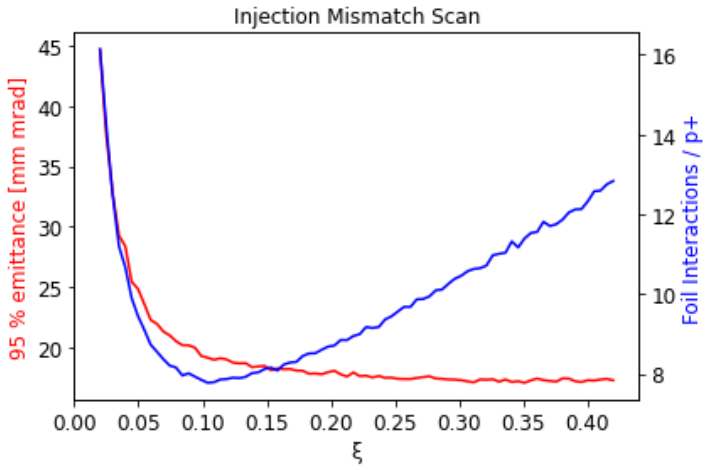

Figure 5: Effect of varying ξ on (blue) Foil Interactions / p+, (red) $\epsilon_{norm}^{95\%}$

Using the PIP-III emittance parameters from Table 1 with Eq. 6 gives $\xi \approx 0.43$. From Fig. 5 it is clear that foil interactions are minimized at $\xi \approx 0.1$, but the $\epsilon_{norm}^{95\%}$ has grown by over 10 %. Conversely, the $\epsilon_{norm}^{95\%}$ rises relatively little from $\xi = 0.43 \rightarrow 0.2$ (<3 %), but the foil interactions are still reduced by more than 40 %. This ξ represents a conservative figure that is more tolerant of error. It was selected to minimize both foil hits and emittance growth. It is also important to note that this injection mismatch only works in regions of small α.

Foil Scattering When a secondary interaction occurs the proton scatters off the foil. There is a well known approximation for small angle scattering. [5] Eq. 7 gives the RMS scattering angle imparted on the proton by the foil. Every time a foil interaction occurs this small angle scattering perturbs the x' and y' of the particle. The ratio $\frac{d_f}{X_C}$ is the thickness of the foil divided by the radiation length of the foil, and it is equal to 1.405 e-5 in the PIP-II CDR. [1]

$$\delta\theta = \frac{13.6 \text{ MeV}}{\beta pc}\sqrt{\frac{d_f}{X_C}}\left[1 + 0.038 \ln \frac{d_f}{X_C}\right] \tag{7}$$

1.3 Simulation Setup

The Python code was written in the Spyder environment and run on a personal computer. Since it tracks particles once per revolution, the time scale of the simulation is written in turns. Particles are injected from a Linac according to the painting functions (Eq. 2 & Eq. 3) and the Gaussian spread of the Linac (Eq. 5). Particles that fall outside of $2.576\sigma_{Linac}$ in both x and y are considered to have not hit the foil and are not tracked. Roughly 99 % of primary particles interact with the foil, all are considered to have been completely stripped. The existing particles are then propagated through Eq. 1, to find their positions at the injection point one turn later. Particles are stored as multidimensional NumPy matrices. To speed up the matrix operations, the Numba package was implemented. The data that is obtained includes the initial and final distribution of the particles in phase space and the position and time of every foil transversal. The MatPlotLib package was used to visualize the data graphically.

1.4 General Injection Studies

These are a few simulations that study the behavior of foil injection.

Accumulation of Secondary Hits A Linac injects particles at a constant current, which means the total amount of particles inside the ring will accumulate following Eq. 8.

$$P(t) = \int_0^t I_{Linac}\, dt = I_{Linac} t \tag{8}$$

The number of secondary interactions per turn is dependent on the number of particles inside the ring. Therefore the total amount of secondary hits accumulates quadratically, shown in Eq. 9 and Fig. 6.

$$\frac{dH(t)}{dt} \propto P(t) \longrightarrow H(t) \propto I_{Linac} t^2 \tag{9}$$

This behavior gets more complex when painting schemes are considered, but it is a good model for displaying how higher Linac currents result in less secondary foil interactions.

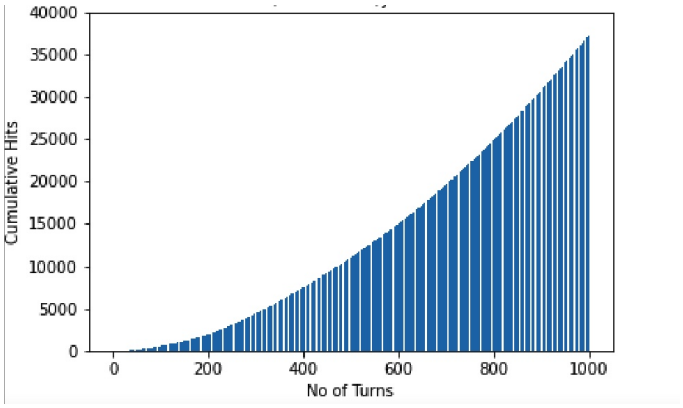

Figure 6: Accumulation of Secondary Hits over Time (Turns)

Foil Size The size of the foil refers to the foil corner, see Fig. 7. The relationship between foil size and secondary hits was investigated to determine if the $2.576\sigma_{Linac}$ used in the PIP-II CDR was optimal. The ratio of stripped particles to injected particles resembles a cumulative distribution function, which makes sense for a Gaussian beam. It shows that for a foil size of 2σ 95 % of the beam is contained. This is because, at 2σ, a particle will have roughly a 2.5 % chance to miss in the x-plane and a 2.5 % chance to miss in the y-plane. Since the x and y distributions are independent, those probabilities simply add. Intuitively, it makes sense that the number of secondary hits would be proportional to the cross sectional area of the foil. Since the foil is a square, the secondary interactions should grow quadratically with foil size. Fig. 7 shows these curves taken from a scan over foil size.

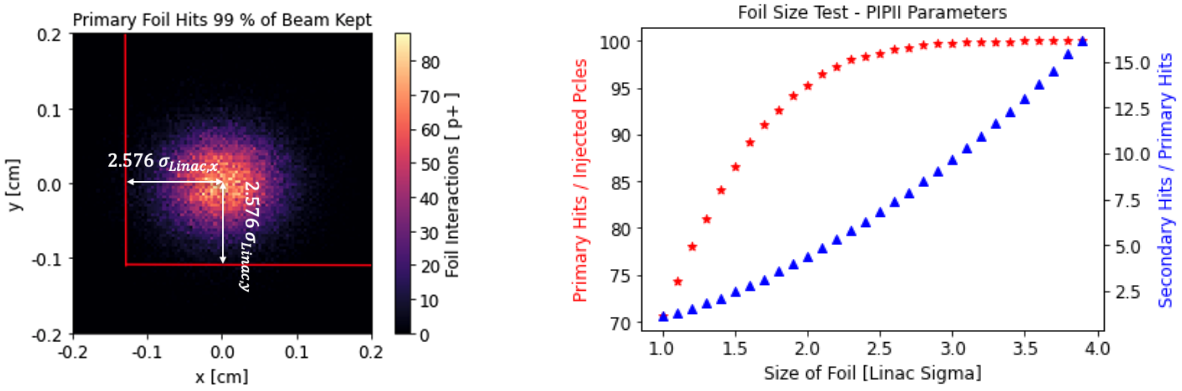

Figure 7: Example of Foil with Primary Hits (left) and Dependence of injection success rate and foil interactions on foil size (right)

To make sure that there was the same number of total protons in each run, the injection times were modified so that foils with lower stripping efficiency ran longer. It turns out that the

$2.576\sigma_{Linac}$ used in the PIP-II CDR is adequate for minimizing unstripped particles, as well as secondary hits. For PIP-II, the number of particles that can miss the foil are constrained by the inline absorber. However, the maximum number of particles that can miss the foil in PIP-III has not been fully determined.

Foil Corner Clipping For certain painting schemes, the highest density of secondary hits occurs at the corner of the foil. A small corner clip could save many secondary interactions. Fig 8 shows how a foil clipping at a distance of 1 mm could potentially save 10 % of foil interactions, without reducing the foil stripping efficiency very much. Furthermore, a combination of the foil cut and foil size can be used to maintain the number of missing particles while reducing secondary hits.

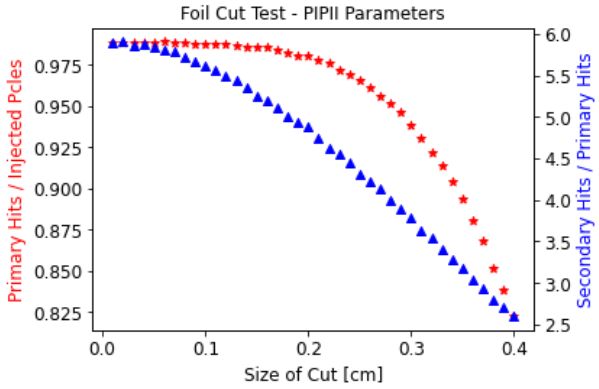

Figure 8: Dependence of injection success rate and foil interactions on foil size

2 PIP-II Simulations

2.1 Simulation Benchmarked against CDR

The foil injection simulations for the PIP-II CDR were written in MathCAD by Valeri Lebedev. [1] The first step in this project was to match these simulations. This was done by implementing the same physics as the CDR simulation but handling data differently. PIP-II implements a anti-correlated transverse painting scheme. Also the injection region for PIP-II has dispersion, which means that the simulation must include longitudinal phase space. The particles were injected longitudinally with a constant momentum offset, as shown in Fig. 9.

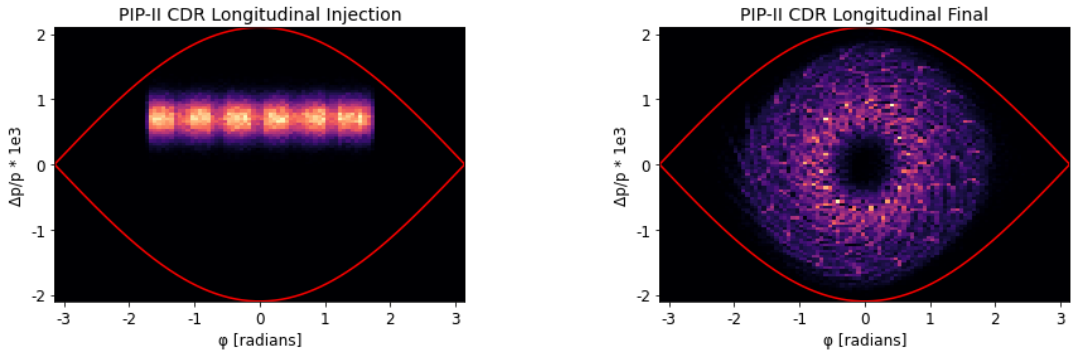

Figure 9: Example of Longitudinal Injection for PIP-II - Initial (left) and Final (right)

The PIP-II CDR MathCAD was used to validate the new simulation, Fig 10 shows how the foil hit profiles are matched well for the two simulations. The PIP-2 CDR cites a peak heating of 63 hits per particle per cm^2 [1], while the new simulation gives a value of 59 hits per particle per cm^2. Actually, the number published in the CDR seems to be on the high side. Rerunning the MathCAD several times typically gave peak values of high 50s to low 60s hits per particle per cm^2. The total number of hits per particle is also similar to within 2 % of each other. The new simulation is well

matched to the MathCAD, which indicates that it is tracking particles accurately. See Table 2 and [1] (Note: This paper calculates hits / p+ whereas the CDR uses secondary hits / p+, these will be off by a factor of exactly 1 as the CDR excludes primary hits)

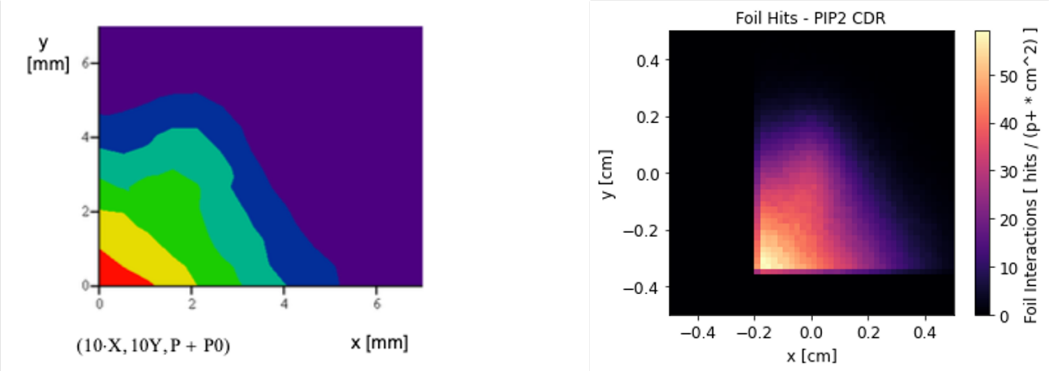

Figure 10: Foil heat-map from the CDR MathCAD simulation (left) and the new simulation (right)

2.2 Optimization of PIP-II Injection

A recent talk was given by Paul Derwent [11] at a joint Proton Source Physics / PIP-II task force meeting on the potential benefits of an on-momentum injection scheme. By adjusting the longitudinal injection for the matched PIP-II CDR simulation, this new injection could be evaluated in terms of its foil hits. Particles were injected with no momentum offset across two ϕ windows. This is easily visualized in Fig. 11.

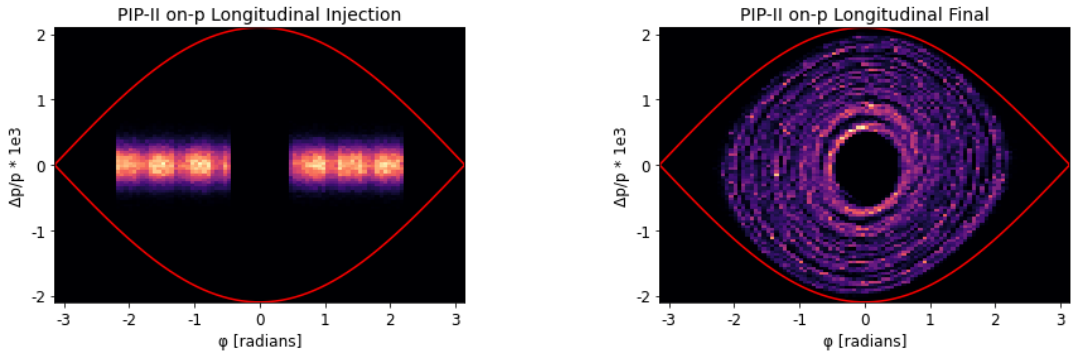

Figure 11: Alternate Longitudinal Injection for PIP-II - Initial (left) and Final (right)

His work indicates that this injection scheme prevents longitudinal beam loss better than the CDR injection scheme. Fig 12 shows a heat-map for all of the hits on the foil. It appears to be

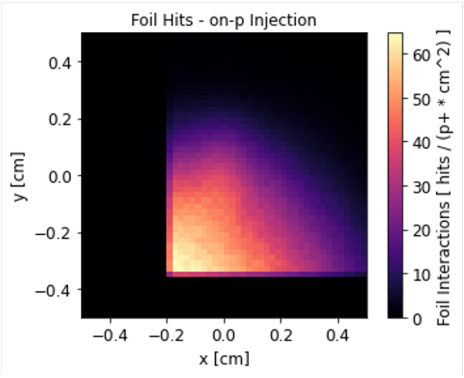

Figure 12: On-momentum foil heat-map showing larger distribution of secondary hits

similar to Fig. 10, but with a greater spread of secondaries on the foil. This simulation showed that the peak hits per particle per cm^2 were roughly 7 % greater and the hits per particle were around 50 % greater for the on-momentum injection scheme. This does not necessarily mean that on-momentum injection is not a viable option. The extra hits may not result in a drastic increase in foil heating because the peak hits per particle per cm^2 is only slightly higher. Also, for PIP-II we are worried more about the particle scattering than the foil heating, since the foil temperature seems to be well below acceptable limits. [1]. To accommodate a goal of fewer hits perhaps a more aggressive injection mismatch could be implemented.

3 2.4 MW Upgrade Simulations

3.1 Simulation Parameters and Results

The PIP-III simulations evolved out of the matched simulation created for PIP-II. However, because the MI-Linac and RCS are planning on injecting into a dispersion free region, dispersive effects from longitudinal painting should not affect the distribution of foil hits. Therefore, these were removed from the PIP-III simulations. Table 1 shows the different injection parameters for the scenarios tested. Table 2 displays the results of the respective simulations. For each PIP-III scenario, simulations were performed with both correlated and anti-correlated painting.

Parameter	PIP-II	RCS-AR	RCS-5mA	MI-Linac
Energy	0.8 GeV	2.0 GeV	~	8.0 GeV
Linac Current	2 mA	2 mA	5 mA	2 mA
Intensity	6.5 e12	36 e12	~	5×36 e12
Pulse Duration	0.52 ms	5×.576 ms	1.15 ms	5×2.9 ms
Revolutions	292	5×286	573	5×260
95% Norm Emit.	16 mm mrad	24 mm mrad	~	24 mm mrad
β_x	20.03 m	33.00 m	~	70.00 m
β_y	6.17 m	24.00 m	~	40.00 m
painting offset$_x$	0.61 cm	1.28 cm	~	1.15 cm
painting offset$_y$	1.10 cm	1.51 cm	~	0.85 cm
ξ	0.48	0.20	~	0.20
Macro Particles	1.75 e5	1.43 e5	~	1.30 e5

Table 1: Parameters for PIP-II & PIP-III Injection

Simulation	Hits / p^+	Pk. Hits / p^+cm^2	Inj. Pt. / p^+cm^2	$\left\langle \text{Hits} / p^+ms \right\rangle$
PIP-II CDR	6.98	60.6	28.9 (14.0)	13.5
PIP-II on-**p**	10.60	64.7	35.4 (20.7)	20.5
5 mA RCS CO	4.24	67.0	47.8 (19.9)	3.69
5 mA RCS AC	6.90	60.6	56.0 (28.3)	6.00
2 mA RCS CO	9.73	172.1	83.5 (55.6)	3.38
2 mA RCS AC	16.92	150.8	105.2 (78.3)	5.88
MI-Linac CO	10.54	320.3	190.3 (151.9)	0.73
MI-Linac AC	18.16	267.8	206.6 (168.5)	1.25

Table 2: Comprehensive Simulation Results

Several different values are given in Table 2. The hits per particle is simply a count of the total foil interactions divided by the number of injected particles. The peak hits per proton per cm^2 is a measure of the greatest hit density per particle on the foil. The injection point per proton per cm^2 measures the hit density per particle at the center of the lianc injection point. The value in parentheses is the contribution to this density from only secondary hits. Finally, the hits per particle per ms is simply the hits per particle divided by injection time for each scenario.

3.2 Optimization of RCS Scenario

RCS 5 mA This scenario assumes that the PIP-II Linac is upgraded to deliver a 5 mA current to the RCS. [6] The higher current allows for the desired beam intensity to be injected in a shorter time frame. Table 2 shows that an anti-correlated injection scheme accumulates roughly 63 % more foil hits over correlated injection. Conversely, the peak density is around 10 % greater for correlated painting. This simulation indicates that correlated painting minimizes secondary hits. However, the anti-correlated painting does give a more even hit distribution. As of now, both painting schemes should still be considered viable options. Fig. 13 shows the foil heat-map for both painting scenarios.

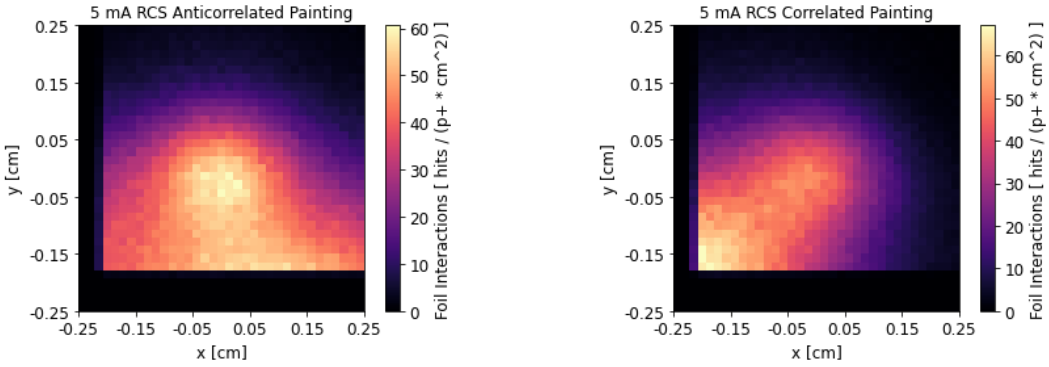

Figure 13: Foil heat-map for anti-correlated (left) and correlated (right) painting on RCS 5 mA

RCS-AR The Accumulator Ring (AR) proposal supposes that the PIP-II Linac will not increase its current beyond 2 mA. In this case, the Linac must inject into an accumulator ring before the RCS. Once the injection is over, the protons can be transferred into the RCS for acceleration. [6] Due to the long injection times required at a lower current, a multi cycle injection is utilized. The painting occurs over five cycles of 286 turns each, i.e every 268 turns the foil is removed and allowed to cool. The cooling time is typically much longer than the injection time, almost two orders of magnitude in [7]. This multi-cycle injection was simulated by removing the foil and allowing the particles to circulate for 50 turns, so that their positions could reach equilibrium when the foil was reinserted and injection was continued. The results of this simulation in Table 2 determine that anti-correlated painting results in about 74 % more foil hits and approximately 12 % less hit density when compared to correlated painting. Again, this scenario seems to favor correlated painting, but anti-correlated still has an advantage in terms of peak heating. Fig. 14 shows the foil heat-map for both painting scenarios. When comparing the foil heat maps, the RCS-AR foil is dominated by secondary hits more so than the 5 mA version.

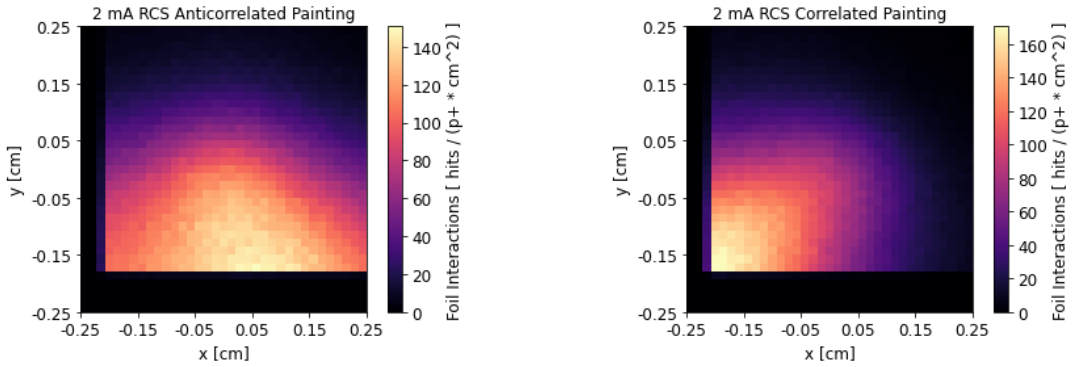

Figure 14: Foil heat-map for anti-correlated (left) and correlated (right) painting on RCS-AR

3.3 Optimization of MI-Linac Scenario

The Main Injector is most extreme foil injection case considered, due to the long injection time and geometric compaction at 8 GeV. Similar to the RCS-AR case, a five cycle painting is considered. A previous study on MI injection [7] found that for uncorrelated painting[1] the foil would see 32.6 hits per particle. The simulated performance of both correlated and anti-correlated painting are an improvement on this previous study; however, once again the correlated painting performs better. From Table 2, anti-correlated painting causes around 72 % more foil hits than a correlated scheme. That said, anti-correlated painting does save over 16 % on hit density. Recall that, reducing foil hits is of greater importance in the MI-Linac than the RCS since the power lost per scattered particle is greater. With this in mind, implementing a correlated painting scheme seems to be advantageous in the MI Linac. Fig. 14 shows the foil heat-map for both scenarios. The high hit density on the foil comes from the relativistic compaction of the beam at 8 GeV. Also, a foil cut could counteract the high concentration of hits at the edge of the correlated foil.

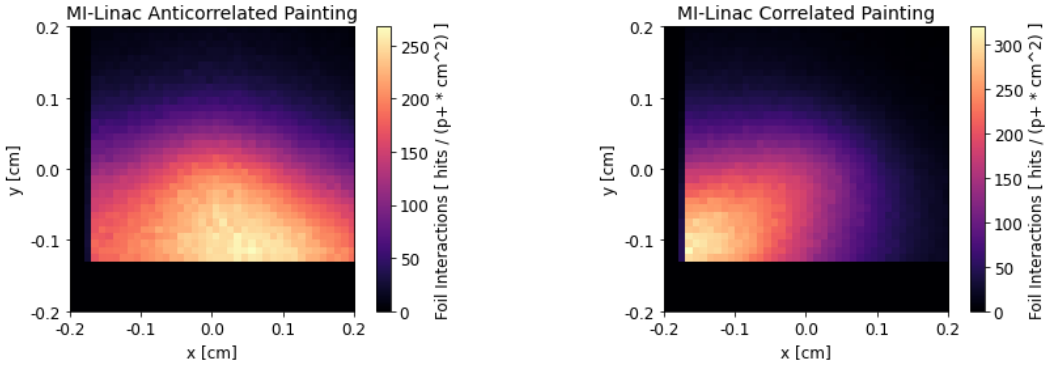

Figure 15: Foil heat-map for anti-correlated (left) and correlated (right) painting on MI-Linac

4 Outlook

The results of theses simulations indicate that correlated painting is ideal for non-dispersive injection, and as injection time grows it becomes even more preferable. This happens because correlated painting moves the foil out of the beam in the most efficient path. The distribution of foil hits in anti-correlated painting was found to be significantly affected by dispersion. Another observation was that for dispersive injection, an on-momentum longitudinal scheme significantly increased the amount of foil injections. Future continuation of this work should include phenomena like space charge and chromaticity. Investigations should be done on emittance growth through transverse coupling. This is important because correlated painting is known to be especially prone to this effect. [3] Errors to the dispersive free region will also effect the distribution through longitudinal painting. As a caveat to this research, laser stripping technology may advance in the coming years into a viable option for PIP-III injection. [8] Despite that possibility, investigations into foil stripping remain important for the future of PIP-III. This upgrade is crucial to the future of Fermilab, and this research provides a baseline of injection performance that can be built on as PIP-III develops over the next decade.

5 Acknowledgements

Firstly, I want to thank my supervisors Jeffrey Eldred and David Neuffer. They were exceptionally supportive and encouraging throughout my internship, and I am grateful that they choose an such an interesting subject matter for my research. Next, I want to thank my group mentors Michael Geelhoed, Ahmed Syed, and Linden Carmichael. They were great in helping me prepare the required presentations. Finally, I want to thank Arden Warner and the entire SIST committee for allowing to participate in this summer internship. This opportunity helped develop skills that will be invaluable to my future science career.

[1] Uncorrelated painting in [7] involved painting across x and y'. This removed particles with large action in both planes.

References

[1] V. Lebedev et al. (PIP-II Collaboration), *The PIP-II Conceptual Design Report*, FERMILAB-TM-2649-AD-APC (2017).
http://pxie.fnal.gov/PIP-II_CDR/PIP-II_CDR_v.0.0.pdf

[2] B. Abi et al. (DUNE Collaboration), *The DUNE Far Detector Interim Design Report Volume 1: Physics, Technology & Strategies*, FERMILAB-DESIGN-2018-02 (2018).
https://arxiv.org/pdf/1807.10334.pdf

[3] J. Beebe-Wang et al. (SNS Collaboration),*Transverse phase space painting for SNS accumulator ring injection*, Proc. of PAC '99, p.1744, (1999).
https://accelconf.web.cern.ch/p99/PAPERS/TUP113.PDF

[4] J. Beebe-Wang and C. R. Prior (SNS Collaboration),*Injection Mismatch for the SNS Accumulator Ring*, BNL/SNS TECHNICAL NOTE NO. 080, (2000).
https://www.bnl.gov/isd/documents/86461.pdf

[5] P.A. Zyla et al. (Particle Data Group), Prog. Theor. Exp. Phys. 2020, 083C01 (2020)

[6] R. Ainsworth et al., *An Upgrade Path for the Fermilab Accelerator Complex*, (2019).
https://arxiv.org/pdf/2106.02133.pdf

[7] A.I. Drozhdin, I.L.Rakhno, S.I. Striganov, and L.G. Vorobiev, *Modeling multiturn stripping injection and foil heating for high intensity proton drivers*, (2012).
https://journals.aps.org/prab/pdf/10.1103/PhysRevSTAB.15.011002

[8] S. Cousineau et al., *High efficiency laser-assisted H^- charge exchange for microsecond duration beams*, (2017).
https://journals.aps.org/prab/pdf/10.1103/PhysRevAccelBeams.20.120402

[9] D.A. Edwards and M.J. Syphers, *Introduction to the Physics of High Energy Accelerators*, Wiley-VCH, (1993).

[10] J.Qiu, J.Y.Tang, S.Wang, and J. Wei,*TRANSVERSE PHASE SPACE PAINTING FOR THE CSNS INJECTION*, Proc. of EPAC'06, (2006).
https://accelconf.web.cern.ch/e06/PAPERS/TUPLS115.PDF

[11] P. Derwent, Booster Injection in the PIP-II era BLonD Simulations, FERMILAB-Beams-doc-9085-v1 (2021).
https://beamdocs.fnal.gov/cgi-bin/sso/ShowDocument?docid=9085